Molecular Dynamics Simulation of Thermomechanical Properties of Hollow Palladium Nanoparticle Pairs during Additive Manufacturing

Ling-Feng Lai,[1] Deng-Maw Lu,[1] and Jian-Ming Lu[2]*

[1]Department of Mechanical Engineering, Southern Taiwan University of Science and Technology,
No. 1, Nantai St., Yungkang Dist., Tainan City 710301, Taiwan
[2]National Center for High-Performance Computing, National Applied Research Laboratories,
No. 28, Nan-ke 3rd Rd., Hsin-Shi Dist., Tainan City 744094, Taiwan

A molecular dynamics (MD) simulation method with the embedded atom model (EAM)/ alloy potential was used to investigate the thermomechanical properties of nanoscale hollow palladium (Pd) nanoparticle pairs during additive manufacturing (AM). The purpose was to explore and analyze hollow Pd nanoparticle pairs at room temperature obtained by AM. The thermomechanical properties of the hollow Pd nanoparticle pairs were discussed with the aim of proposing optimal parameters. It was shown that the nanoscale coalescence temperature of Pd was in the range of 750 to 1530 K and the nanoscale melting temperature was from 1414 to 1600 K, which were much lower than the macroscopic melting point (1828.05 K) of Pd. It was found that solid-state sintering can occur spontaneously at room temperature. The size and geometrical structure of the nanoparticles and the heating rate played important roles during AM.

1. Introduction

Additive manufacturing (AM) technologies[1–3] were divided into seven categories of technology by the American Society for Testing and Materials International (ASTM) in 2009. Among them, metallic AM[4] can be subdivided into four types: powder bed fusion,[5–7] binder jetting,[8] sheet lamination, and direct energy deposition.[9] Metallic AM technology is more difficult to use in manufacturing than the others. The materials, structure, strength, thermodynamic parameters, stress, and strain are all key parameters of AM. The AM methods include sintering, bonding, melting solidification, and vapor deposition; the design concept can be drawn as a 3D model through computer-aided software; and the AM parameters such as the numbers of slice layers and support structures, temperature, and printing speed can be set. AM technologies have been applied to microsensors, the surface plating of special sensing material layers, aerospace, machinery, biomedicine, architecture, art design, and so forth.

The manufcturing methods of metallic powders include atomization, electrolytic deposition, reduction, granulation, the use of prealloyed powders, the use of precoated powders, machining, and milling. The sizes and shapes of metallic microparticles and nanoparticles obtained by the above methods are different.

The formation methods of metallic nanopowders include gravity sintering, centrifugal compacting, pressing, extruding, slip casting, rolling, isopressing, isostatic molding, explosive compacting, and fiber metal processing. After the metallic nanopowder is formed, room-temperature cooling, nitrogen cooling, or liquid nitrogen cooling is used. Afterwards, a thin film is coated on the surface of the metallic nanoparticles to prevent their oxidation, because some metallic materials cannot undergo a reduction–oxidation reaction after oxidation.

In general, after the coating of metallic nanoparticles, nonspherical metallic nanoparticles, such as cutting balls, flattened balls, double balls, collisions, ellipsoids, and water droplets, are removed, and the metallic nanoparticles that exceed the required size are removed by sieving to improve their quality. In this study, we focus on hollow palladium (Pd) nanoparticles because they can be used to improve the performance of nanosensors, microsensors, and sensing film materials used in AM technology.

Pd has both the lowest melting temperature and the lowest density among the platinum group metals. It is used in thin-film gas sensors, catalytic converters, aircraft spark plugs, surgical instruments, and jewelry and as a dental implant material. In the present study, we simulated the thermomechanical properties of hollow spherical Pd nanoparticle pairs, and we found the optimal parameters under different heating parameters during laser powder bed fusion AM.

## 2.	Materials and Methods

### 2.1	Molecular dynamics (MD) simulations

MD[10–12] is based on Newton's laws of mechanics and is used to simulate the motion and travel trajectories of Pd atoms, the force, and the changes in atomic structure. We used MD simulation to determine the thermomechanical properties of nanoscale Pd.

Large-scale atomic/molecular massively parallel simulator (LAMMPS)[13–15] is an open-source MD program. It is based on the GPL open-source code and written in C language to support parallel, single-processor, and multiple-processor computing, and so forth. Therefore, we utilized LAMMPS to simulate Pd nanoparticle pairs.

In this paper, LAMMPS is used to investigate hollow spherical Pd nanoparticle pairs under different parameters in AM to observe their thermomechanical properties and to find the optimal parameters for hollow spherical Pd nanoparticles.

### 2.2	Atomic model preparation

We set the simulation environment range to be larger than that of hollow spherical Pd nanoparticle pairs. In the examined system, the initial temperature was set to 300 K, the simulation step was set to 2 fs, nonperiodic boundary conditions were set, and the environment

was set as the constant-temperature, constant-volume ensemble (NVT), also referred to as the canonical ensemble. The embedded atom model (EAM)/alloy potential form and the Velocity Verlet integration method were used. The lattice structure of Pd was set to 3.8904 Å, that of face-centered cubic (fcc) Pd,[16,17] and the initial gap between two nanoparticles in the pair was set to 5 Å in LAMMPS. The heating temperature was linearly increased from 300 to 2100 K. After several test simulations, the shell thickness of the hollow spherical Pd nanoparticles was set to 4 Å, which was close to the minimum thickness of a hollow Pd nanoparticle. We set three nanoparticle diameters (16a, 20a, and 24a), three groups of the same nanoparticle size, and three groups of different nanoparticle sizes, as shown in Table 1 and Fig. 1. The heating rate was set to 1, 0.5, and 0.25 K/ps.

2.3　Auxiliary analysis and calculation

LAMMPS with the EAM/alloy potential[18] can describe the atomic interaction forces,[19] positions, and trajectories of hollow spherical Pd nanoparticles at each time step in metallic AM, where the electron density was obtained from the wave function. The atoms required to be calculated for each atomic energy were then embedded in the local electron density energy range.[20] The whole fitting procedure was proposed in an earlier study.[21]

The Velocity Verlet algorithm was integrated to obtain the positions, velocities, and physical quantities of the atoms of the hollow spherical Pd nanoparticles. The canonical ensemble (NVT) was the ensemble that represents the possible states in thermal equilibrium at a fixed temperature. Under the spatial constraints of the environment, the total number of atoms (N),

Table 1
Description of hollow Pd nanoparticle pairs.

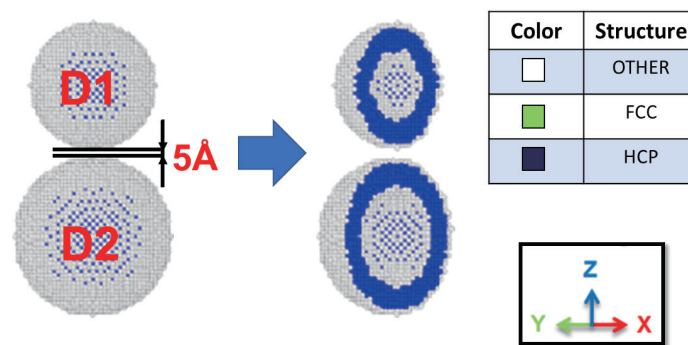| D1	D2	Atoms
16a	16a	15056
20a	20a	26336
24a	24a	40616
16a	20a	20696
16a	24a	27836
20a	24a	33476

Fig. 1.　(Color online) Cross-sectional view of hollow Pd nanoparticle pairs.

temperature (T), pressure (P), volume (V), and energy (E) balance in the environment. The neck width was the distance between the outermost parts of two hollow spherical Pd nanoparticles at room temperature.

Common neighbor analysis (CNA)[22] was used to simulate the hollow spherical Pd nanoparticles in metallic AM and visualize each lattice structure at each time step. The color of Pd atoms in the disordered atomic structure was white (HTML:#ffffff), the color of the fcc structure was green (HTML:#66ff66), and the color of the hexagonal close-packed (hcp) structure was blue (HTML:#00007f).

The gyration radius (R_g) [Eq. (1)] was used to calculate the root mean square distance between the atoms and the center of mass of the hollow spherical Pd nanoparticles in metallic AM. The total mass of the simulated environment space was set to M, the center of mass of an atom was set to r_{cm}, the position of each atom in the nanoparticle was set to r, and the subscript i in Eq. (1) was used to denote all atoms in the environment.[23]

$$R_g^2 = \frac{1}{M}\sum_i m_i \left(r_i - r_{cm}\right)^2 \tag{1}$$

By analyzing the mean square displacement (MSD) [Eq. (2)], we obtained the initial position, final position, and average displacement of all the atoms inside the hollow spherical Pd nanoparticle pairs in the metallic AM process. The total mass of the space was set to N, the time was set to t, the position of each atom in the nanoparticles was set to r, and the subscript i in Eq. (2) was used to denote all atoms in the space.[24,25]

$$MSD = \frac{1}{N}\sum_i \left(r_i(t) - r_i(0)\right)^2 \tag{2}$$

3. Results and Analysis

3.1 Thermal equilibration at room temperature

In the present paper, the MD process consists of three stages: relaxation, thermal equilibrium, and laser sintering. First, the hollow spherical Pd nanoparticle pairs were heated for 1000 ps at 300 K. When the hollow spherical Pd nanoparticle pairs were constructed and the internal atoms were artificially removed, internal stress was generated, making it necessary for them to be heated to relax the internal stress and adjust the inner and outer surface tension of the hollow spherical Pd nanoparticle pairs and the fcc structure of the Pd. Thus, the lattice was distorted and the internal stress was relieved.

LAMMPS was used to analyze the hollow spherical Pd nanoparticle pairs at room temperature not heated by the laser. Six combinations (16a–16a, 20a–20a, 24a–24a, 16a–20a, 16a–24a, and 20a–24a in Table 1) were observed, and the Pd nanoparticles were all self-sintered and coalesced owing to the nanoscale size effect.

We take the 16a–20a hollow spherical Pd nanoparticle pairs as the reference example to explain the thermomechanical behaviors of the hollow spherical Pd nanoparticle pairs. Points a, b, c, and d in Fig. 2 correspond to the changes in the hollow spherical Pd nanoparticle pairs at different time steps. At Point a, the initial gap of the hollow spherical Pd nanoparticle pairs is 5 Å, the radius of gyration is 46.70 Å, the neck width is 0 Å, fcc accounts for 66.97%, hcp accounts for 0%, and other structures account for 33.03%. At Point b, the Pd nanoparticle pairs self-sinter and coalesce owing to the nanoscale size effect, and the neck width rapidly increases. At Point b, the radius of gyration is 46.69 Å, the neck width is 27.18 Å, fcc accounts for 66.77%, hcp accounts for 0.05%, and other structures account for 33.18%. The hollow spherical Pd nanoparticle pairs coalesce to increase the content of the disordered atomic structure to its highest value. At Point c, the radius of gyration is 66.26 Å, the neck width is 36.79 Å, fcc accounts for 66.77%, hcp accounts for 0.28%, and other structures account for 33.46%. At Point d, the internal atomic structure of the hollow spherical Pd nanoparticle pairs reaches the equilibrium state and the neck width stabilizes. The radius of gyration is 46.63 Å, the neck width is 35.25 Å, fcc accounts for 66.70%, hcp accounts for 0.57%, and other structures account for 32.73%.

3.2 Laser sintering

LAMMPS was used to model the hollow spherical Pd nanoparticle pairs in the metallic AM process. The hollow spherical Pd nanoparticles were heated by a laser, causing their internal atomic structure to change. The atomic structure, force, trajectory, and thermomechanical properties were observed at different time steps. The system was gradually heated from 300 to 2100 K at heating rates of 0.25, 0.5, and 1 K/ps. Laser sintering was divided into four stages
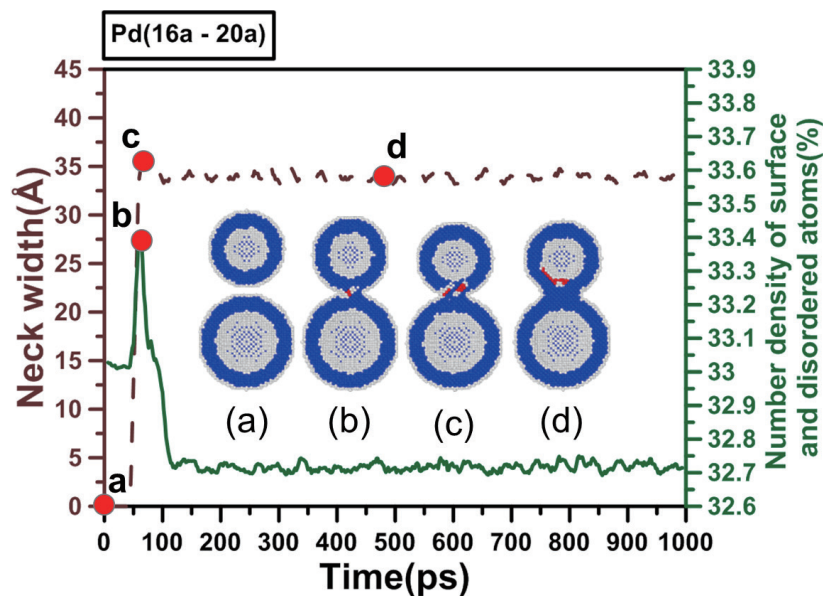

Fig. 2.   (Color online) Time histories of neck width and number density of surface and disordered atoms for cross-sectional view of 16a–20a hollow Pd nanoparticle pairs.

under different time steps: a relatively stable stage, a coalescence stage, a melting stage, and a completely melted stage.

In Fig. 3, we use the 16a–20a hollow spherical Pd nanoparticle pairs as an example to explain the thermomechanical behaviors of the hollow spherical Pd nanoparticle pairs at 0.25 K/ps. From Point A to Point C in Fig. 3, the hollow spherical Pd nanoparticles are in a relatively stable state; from Point C to Point D under gradual heating, the hollow spherical Pd nanoparticle pairs begin to coalesce (coalescence stage); from Point D to Point E, the hollow Pd spherical nanoparticles begin to melt into a metallic liquid, causing their internal structure to change relatively abruptly (melting stage). After Point E, the hollow spherical Pd nanoparticles are completely melted into a metallic liquid (completely melted stage).

In Fig. 4, we use the 16a–20a hollow spherical Pd nanoparticle pairs as an example to explain the temperature dependence of the MSD for the hollow Pd nanoparticle pairs at three laser heating rates. It was found that the Pd atoms start to diffuse at 1175 K at a heating rate of 1 K/ps, at which the MSD of the Pd atoms is 1530 $Å^2$.

Figure 5 shows the temperature dependence of the MSD for the hollow Pd nanoparticle pairs at the heating rate of 1 K/ps. It was found that the atomic diffusion temperature of hollow Pd nanoparticle pairs is between 910 and 1200 K, and that the MSD of Pd atoms is between 1320 and 2150 $Å^2$. Figure 6 shows the temperature dependence of the MSD for the hollow Pd nanoparticle pairs at the heating rate of 0.5 K/ps. The atomic diffusion temperature of the hollow Pd nanoparticle pairs is between 825 and 1105 K, and the MSD of Pd atoms is between 1841 and 3112 $Å^2$. Figure 7 shows the temperature dependence of the MSD for the hollow Pd nanoparticle pairs at the heating rate of 0.25 K/ps. The atomic diffusion temperature of the hollow Pd nanoparticle pairs is between 770 and 990 K, and the MSD of Pd atoms is between 2216 and 4179 $Å^2$.
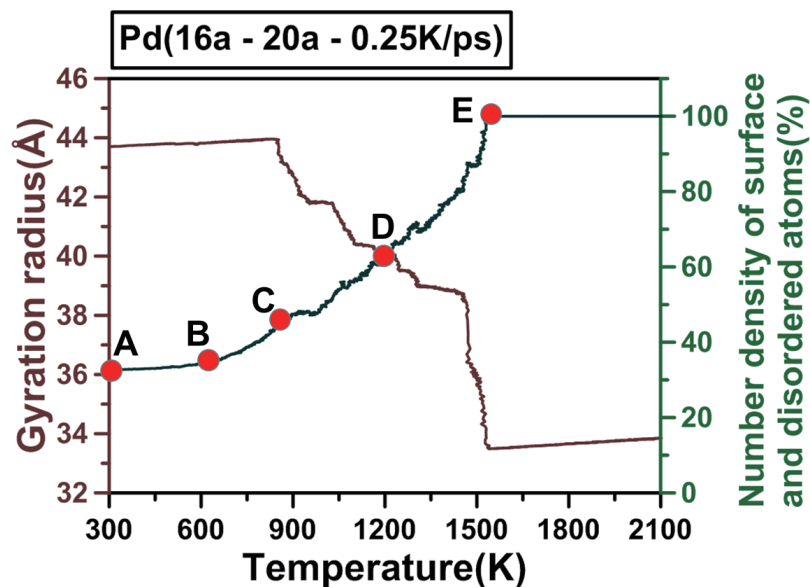

Fig. 3.   (Color online) Temperature dependence of the gyration radius and number density of surface and disordered atoms for the hollow Pd nanoparticle pairs with diameters of 16a and 20a (heating rate of 0.25 K/ps).
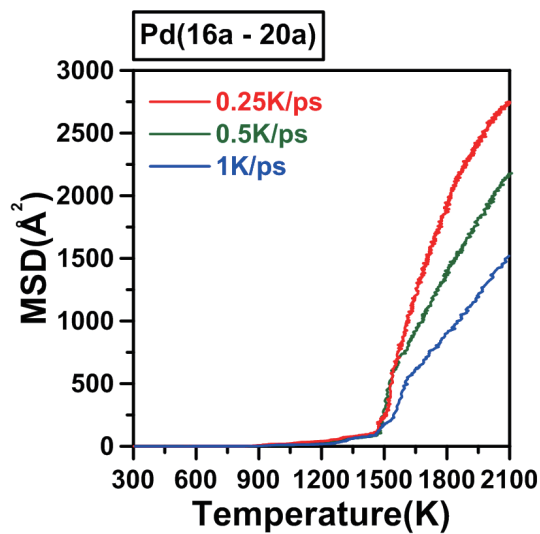
Fig. 4. (Color online) Temperature dependence of the MSD for the hollow Pd nanoparticle pairs with diameters of 16a and 20a at three laser heating rates.
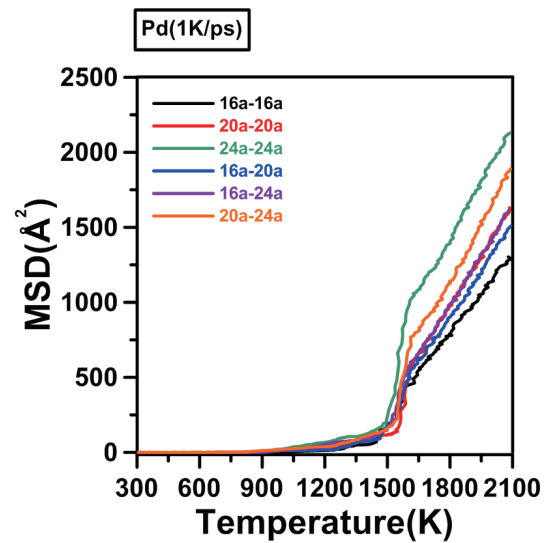

Fig. 5. (Color online) Temperature dependence of the MSD for the hollow Pd nanoparticle pairs at 1 K/ps.
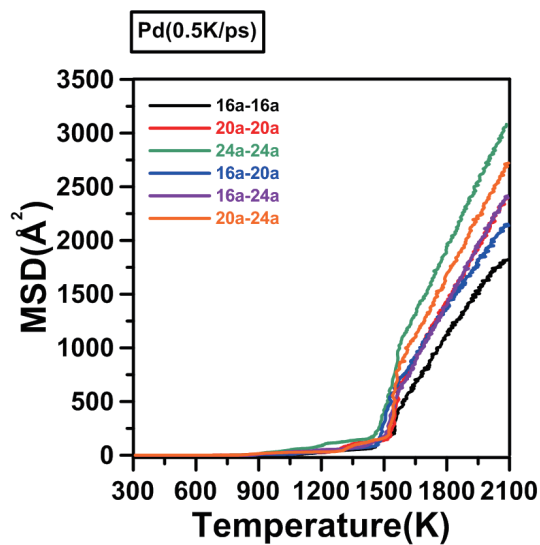

Fig. 6. (Color online) Temperature dependence of the MSD for the hollow Pd nanoparticle pairs at 0.5 K/ps.
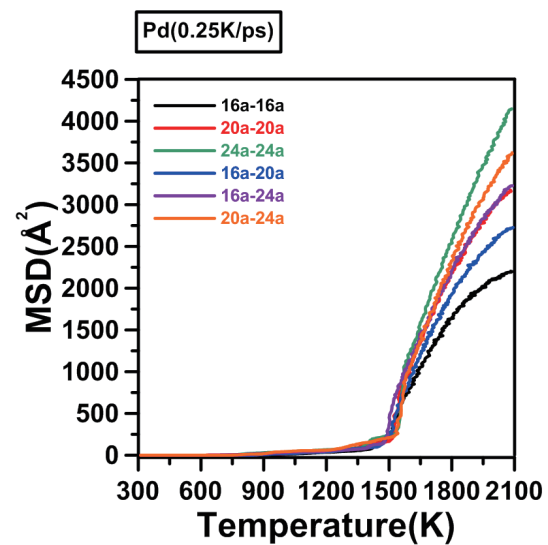

Fig. 7. (Color online) Temperature dependence of the MSD for the hollow Pd nanoparticle pairs at 0.25 K/ps.

According to Figs. 5–7, the onset temperature and MSD of the 20a–20a and 16a–24a hollow Pd nanoparticle pairs are relatively similar regardless of the heating rate. The onset temperature of the 20a–20a hollow Pd nanoparticle pairs is 910 K and the MSD is 1655 $Å^2$ at 1 K/ps. The onset temperature of the 20a–20a hollow Pd nanoparticle pairs is 825 K and the MSD is 2425 $Å^2$ at 0.5 K/ps. The onset temperature of the 20a–20a hollow Pd nanoparticle pairs is 861 K and the MSD is 3224 $Å^2$ at 0.25 K/ps.

Figures 5–7 also show that the onset temperature of the 16a–24a hollow Pd nanoparticle pairs is 910 K and the MSD is 1645 Å^2 at 1 K/ps. The onset temperature of the 16a–24a hollow Pd nanoparticle pairs is 825 K and the MSD is 2435 Å^2 at 0.5 K/ps. The onset temperature of the 16a–24a hollow Pd nanoparticle pairs is 770 K and the MSD is 3250 Å^2 at 0.25 K/ps.

In Figs. 5–7, it was found that the greatest displacement of Pd atoms occurs when the MSD curve changes rapidly. The starting diffusive temperature of the Pd atoms is highest at a heating rate of 1 K/ps. The atomic diffusive trajectory of Pd is the most uniform and the MSD reaches its highest value at a heating rate of 0.25 K/ps.

From the auxiliary analyses of the cut-off radius and the potential energy of Pd, we found that the coalescence temperature of the hollow spherical Pd nanoparticle pairs is between 750 and 1530 K, as shown in Fig. 8, where the error bars indicate the temperature range in which rapid neck growth occurs. Figure 8 shows that the coalescence temperatures of the 16a–20a hollow spherical Pd nanoparticle pairs are between 859 and 1414 K at 1 K/ps, between 859 and 1465 K at 0.5 K/ps, and between 859 and 1465 K at 0.25 K/ps.

From the auxiliary analyses of the cut-off radius and the potential energy of Pd, we found that the melting temperature of the hollow spherical Pd nanoparticle pairs was between 1414 and 1600 K, as shown in Fig. 9, where the error bars indicate the range of melting temperatures, with the symbols located at their centers. Figure 9 shows that the melting temperature of hollow spherical Pd nanoparticle pairs of 16a–20a is between 1414 and 1600 K at 1 K/ps, between 1465 and 1565 K at 0.5 K/ps, and between 1465 and 1565 K at 0.25 K/ps. Figure 9 also shows that the melting temperature of the nanoscale Pd was much lower than that of macroscopic Pd (1828.05 K).
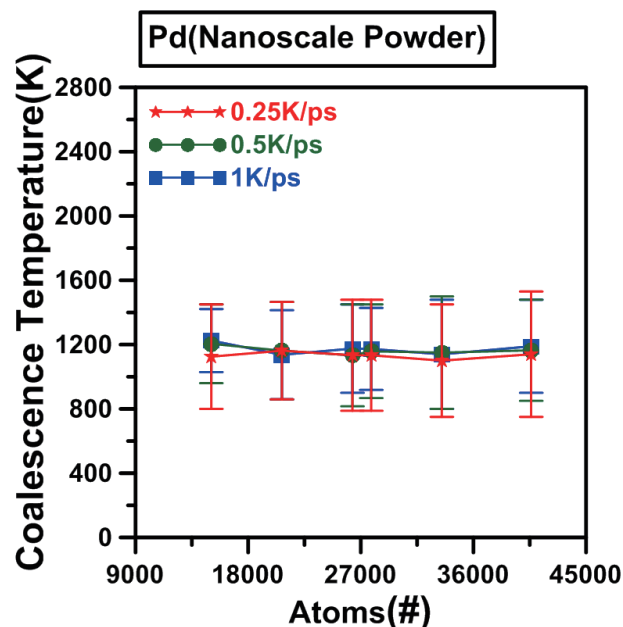

Fig. 8. (Color online) Coalescence temperature as a function of heating rate for hollow Pd nanoparticle pairs with three laser heating rates. The error bars indicate the temperature range in which rapid neck growth occurs.
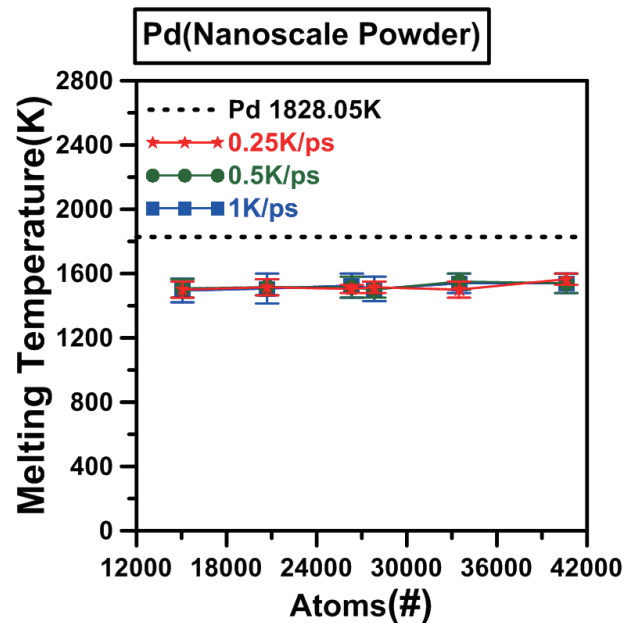
Fig. 9.　(Color online) Melting temperature as a function of number of atoms for Pd nanoparticle pairs with three laser heating rates. The error bars indicate the range of melting temperatures, with the symbols located at their centers. The dotted line is the macroscopic melting point of Pd (1828.05 K).

When the heating rate of hollow spherical Pd nanoparticle pairs was 1 K/ps, the atomic diffusive temperature was between 910 and 1200 K and the MSD of atomic diffusion was 1320–2150 $Å^2$. When the heating rate was 0.5 K/ps, the atomic diffusive temperature was between 825 and 1105 K and the MSD of atomic diffusion was 1841–3112 $Å^2$. When the heating rate was 0.25 K/ps, the atomic diffusive temperature was between 770 and 990 K and the MSD of atomic diffusion was 2216–4179 $Å^2$.

4.　Conclusions

We observed the thermomechanical properties of nanoscale Pd under different AM parameters. The coalescence temperature of Pd nanoparticles was found to be between 750 and 1530 K, and the melting temperature of Pd nanoparticles was found to be between 1414 and 1600 K. It was concluded that the coalescence and melting temperatures of hollow spherical Pd were much lower than the melting point of macroscopic Pd (1828.05 K). The solid-state sintering of hollow spherical Pd can occur spontaneously at room temperature. Our results indicate that the size and geometrical structure of nanoparticles and the heating rate play important roles during the AM process.

Acknowledgments

References

1 A. Bacciaglia, A. Ceruti, and A. Liverani: Procedia Comput. Sci. **200** (2022) 1113. https://doi.org/10.1016/j.procs.2022.01.311
2 J. Contreras-Naranjo, V. Perez-Gonzalez, M. Mata-Gómez, O. Aguilar: Electrochem. Commun. **130** (2021) 107098. https://doi.org/10.1016/j.elecom.2021.107098
3 I. Tomaz, S. Uí Mhurchadha, S. Marques, P. Quinn, H. Funke, F. Birkholz, S. Zietzschmann, and R. Raghavendra: Addit. Manuf. Lett. **1** (2021) 100004. https://doi.org/10.1016/j.addlet.2021.100004
4 W. E. Frazier: J. Mater. Eng. Perform. **23** (2014) 1917. https://doi.org/10.1007/s11665-014-0958-z
5 M. A. Obeidi, A. Conway, A. Mussatto, M. N. Dogu, S. Sreenilayam, H. Ayub, I. Ahad, and D. Brabazon: Addit Manuf. **13** (2022) 100264. https://doi.org/10.1016/j.rinma.2022.100264
6 R. Yavari, A. Riensche, E. Tekerek, L. Jacquemetton, H. Halliday, M. Vandever, A. Tenequer, V. Perumal, A. Kontsos, Z. Smoqi, K. Cole, and P. Rao: Mater. Des. **211** (2021) 110167. https://doi.org/10.1016/j.matdes.2021.110167
7 M. Binder, L. Kirchbichler, C. Seidel, C. Anstaett, G. Schlick, and G. Reinhart: Procedia CIRP **81** (2019) 992. https://doi.org/10.1016/j.procir.2019.03.240
8 A. Foroozmehr, M. Badrossamay, E. Foroozmehr, and S. Golabi: Mater. Des. **89** (2016) 255. https://doi.org/10.1016/j.matdes.2015.10.002
9 A. Mostafaei, A. Elliott, J. Barnes, F. Li, W. Tan, C. Cramer, P. Nandwana, and M. Chmielus: Prog. Mater. Sci. **119** (2021) 100707. https://doi.org/10.1016/j.pmatsci.2020.100707
10 J. Jeon, S. Jiang, F. Rahmani, and S. Nouranian: J. Nanopart. Res. **22** (2020) 26. https://doi.org/10.1007/s11051-019-4747-3
11 S. Jiang, Y. Zhang, Y. Gan, Z. Hen, and H. Peng: J. Phys. D: Appl. Phys. **46** (2013) 33. https://doi.org/10.1088/0022-3727/46/33/335302
12 S. Hartmann, O. Hölck, and B. Wunderle: Procedia Mater. Sci. **3** (2014) 454. https://doi.org/10.1016/j.mspro.2014.06.076
13 F. Rahmani, J. Jeon, S. Jiang, and S. Nouranian: J. Nanopart. Res. **20** (2018) 133. https://doi.org/10.1007/s11051-018-4237-z
14 A. P. Thompson, H. M. Aktulga, R. Berger, D. Bolintineanu, W. M. Brown, P. Crozier, P. Veld, A. Kohlmeyer, S. Moore, T. D. Nguyen, R. Shan, M. Stevens, J. Tranchida, C. Trott, and S. Plimpton: Comput. Phys. Commun. **271** (2022) 108171. https://doi.org/10.1016/j.cpc.2021.108171
15 S. Melin, P. Hansson, and A. Ahadi: Procedia Struct. Integrity **23** (2019) 137. https://doi.org/10.1016/j.prostr.2020.01.076
16 J. Zhang, G. Liu, and J. Sun: Nano Mater. Sci. **2** (2020) 58. https://doi.org/10.1016/j.nanoms.2019.11.002
17 Y. Guo, Z. Wang, B. Zhang, J. Teng, W. Zeng, Y. Zhao, L. Fu, D. Li, Y. Ma, W. Song, L. Liu, Z. Zhang, X. Yan, L. Wang, Y. Zhu, and X. Han: Cell Rep. Phys. Sci. **3** (2022) 100736. https://doi.org/10.1016/j.xcrp.2021.100736
18 R. Bodlos, V. Fotopoulos, J. Spitaler, A. L. Shluger, and L. Romaner: Materialia **21** (2022) 101362. https://doi.org/10.1016/j.mtla.2022.101362
19 T. Deguchi, T. Nakahara, K. Imamura, and N. Ishida: Adv. Power Technol. **32** (2021) 30. https://doi.org/10.1016/j.apt.2020.11.011
20 M. Garrett and C. Race: Comput. Mater. Sci. **188** (2021) 110149. https://doi.org/10.1016/j.commatsci.2020.110149
21 R. Johnson: Phys. Rev. B. **37** (1988) 6121. https://doi.org/10.1103/PhysRevB.37.6121
22 W. Polak: Comput. Mater. Sci. **201** (2022) 110882. https://doi.org/10.1016/j.commatsci.2021.110882
23 K. Haydukivska, V. Blavatska, and J. Paturej: Sci. Rep. **10** (2020) 14127. https://doi.org/10.1038/s41598-020-70649-z
24 X. Michalet: Biophys. J. **100** (2011) 252a. https://doi.org/10.1016/j.bpj.2010.12.1593
25 P. Geslina and D. Rodney: J. Mech. Phys. Solids **153** (2021) 104479. https://doi.org/10.1016/j.jmps.2021.104479

About the Authors

Ling-Feng Lai received her B.S. and M.S. degrees from Chia Nan University of Pharmacy & Science, Taiwan, in 2015 and 2018, respectively. Since 2018, she has been a Ph.D. student at Southern Taiwan University of Science and Technology, Taiwan. Her research interests include the molecular dynamics simulation of additive manufacturing. (da71y201@stust.edu.tw)

Deng-Maw Lu received his B.S. degree from Tamkang University, Taiwan, in 1979 and his M.S. and Ph.D. degrees from National Cheng Kung University in 1985 and 1996, respectively. From 1985 to 1988, he was a lecturer at Southern Taiwan University of Science and Technology, Taiwan. Since 1988, he has been a professor. His research interests are in creative mechanism design, mechanical design, nanotechnology and simulation, and the history of science. (dmlu@stust.edu.tw)

Jian-Ming Lu received his Ph.D. degree from National Cheng Kung University, Taiwan, in 2008. He has been a research fellow since 2015 and was an associate researcher at National Center for High-Performance Computing in Taiwan from 2004 to 2015. His major research interests are in the molecular dynamics of nanomaterials, namely, carbon nanotubes, graphene, and graphene; nanodevices, and the additive manufacturing of nanoscale pure metal and high-entropy alloys. (0403817@narlabs.org.tw)